Indian Journal of Engineering & Materials Sciences
Vol. 26, October-December 2019, pp. 298-310

Analysis and characterization of weld quality during butt welding through friction stir welding

Ankit Kumar Pandey[a], Suman Chatterjee[b*] & Siba Sankar Mahapatra[b]

[a]Indian Institute of Technology, Bombay 400 076, India

[b]National Institute of Technology, Rourkela 769 008, India

Received 08 June 2018; Accepted 26 July 2019

In the present study, butt weld produced by friction stir welding of aluminium 1060 alloy has been analyzed. Destructive test, non-destructive test, and SEM image analysis methods have been implemented to investigate the microstructural evolution and mechanical properties of welded joints. The effects of tool rotation speed, welding speed, tool pin profile and tool offset have been investigated to optimize welding conditions for required weld properties. Face-centered central composite design of response surface methodology has been adapted to analyze the effect of parameters with an optimal number of experiments. It has been observed that weld produced with threaded pin tool has higher ultimate tensile stress and ultimate flexural stress. Radiography test has shown that cracks are not present in the produced weldment. From the study of the fracture surface of the tensile test specimen, it has been found that ductility of weld is highest at the top area and decreases towards the bottom area of weld. Dimple formation has been found at the top area of the fracture surface but has been absent in the bottom area of weld. Vickers hardness of weld zone and the heat affected zone has found to be less than the base material.

Keywords: Friction stir welding, Non-destructive testing, Response surface methodology, Mechanical properties, Micro structural evolution

1 Introduction

Aluminium and its alloys are one of the most widely used materials in the present world[1]. Its application is widely spread in the field of the automobile industry, aerospace industry, infrastructure, and navy. It is predicted that use of these materials will rise in future[2,3]. Aluminium 1060 alloy finds many applications due to lightweight, good ductility, good malleability and corrosion resistance properties. But conventional welding is not used for welding of these materials due to the formation of defects like porosity, lack of fusion and burn through[1]. Friction stir welding (FSW) is a new promising welding technique invented by The Welding Institute (TWI) in the early 1990's[4]. FSW is a solid-state welding technique which produces weld by mixing of workpiece material at an elevated temperature. As it is a solid state welding technique, weld joints are free from defects arising due to melting of material. By this process, aluminium alloys welding can also be produced with similar benefit[5]. Mishra *et al.*[6] have described the FSW process, the mechanism responsible for the FSW and the effect of different parameters on weld produced.

Shrivastava *et al.*[7] have found that the FSW consumes less energy as compared to conventional arc welding process. Ericsson *et al.*[8] have showed that MIG and TIG welds show lower static and dynamic strength than FSW welds. Li *et al.*[9] have concluded that notch tensile strength and notch strength ratio of friction stir welding are higher than TIG welding process. Carlone *et al.*[10] have reported that grain refinement is achieved in the nugget zone of FSW, which increases the weld strength. Khodaverdizadeh *et al.*[11] have discussed the strain hardening behavior by dislocation density and grain size variation during FSW. Silva *et al.*[12] have concluded that FSW can be used to improve fatigue strength of weld joints. Chen *et al.*[13] have successfully joined small dimension, thin Al-alloy and Cu pipes with two offsets and showed the versatility of the process.

Many authors have contributed to establish that the quality of weld produced by FSW depends on the parametric setting used for producing the weld[14]. Tool rotation speed, welding speed, offset of the tool from weld line, tool tilt angle and the vertical pressure are some of the parameters which can affect the joint produced. The peak temperature generated during welding increases with the increase in tool rotation

*Corresponding Author (E-mail: mrsumanmech@gmail.com)

speed but decreases slightly with increase in welding speed[11]. Zhang *et al.*[15] observed that pin diameter followed by rotational speed significantly influence on tensile strength of welded joints. Xue *et al.*[16] have reported that a larger pin offset towards Al in the advancing side leads to a sound defect free joints in Al-Cu joint. Dwivedi *et al.*[17] has shown that the lower axial force, higher welding speed and higher tool rotation speed produces better weld strength with less defects. Peel *et al.*[18] have observed that micro structure change resulting from welding speed causes change in hardness at the weld zone. Sakthivel *et al.*[19] have shown that better mechanical properties can be achieved at lower transverse speed due to higher heat input to the weld zone. The ductility of the weld can be increased by post welding heat treatment[20]. Beygi *et al.*[21] have considered Al-Cu bilayer sheet produced by cold rolling and observed that materials flow upwards in the advancing side and downwards in the retreating side. Tan *et al.*[22] have confirmed that a layered structure consisting of composite gives excellent metallurgical bonding to the weld. Donatus *et al.*[23] have concluded that materials flow more from the advancing side to the retreating side. Xu *et al.*[24] have shown the microstructural difference at different zones of weld nugget. The finest grains were found in the region closest to the tool edge. Nadan *et al.*[14] have shown that FSW process is quite uncertain and causes some variation in weldment even at same parametric condition.

As described before, in FSW process tool is a non-consumable body which produces the weld. Tool geometry plays a vital role in material flow around the tool. Li *et al.*[25] have shown that weld profile and bonding width of the weld zone differs with the tool profile. Su *et al.*[26] have observed that the interaction between the tool and work piece affects the thermal properties, plastic deformation and recrystallization of the material. Jesus *et al.*[27] have developed different tool geometrics and their effect on the weld morphology has been estimated. Trueba *et al.*[28] have observed that the shoulder size should be optimal to get best strength. It has been shown that during the material flow, the material flows mainly in the retreating side[29-31]. Zhao *et al.*[32] have studied different tool pin effects on the weld produced. Taper threaded tool produced a sound defect-free weld. Schmidt *et al.*[33] and Guerra *et al.*[34] have studied effect of different tools and concluded that threaded tool produces more heat and improve flow of softer material by exerting a downward force. Buffa *et al.*[35] have studied the effect of pin angle (angle between the pin axis and conical surface) and observed that increasing the angle leads to more uniform temperature distribution along the vertical direction which reduces the distortion of work piece.

In the present study, two parts of six millimeters size aluminium 1060 alloy have been welded using FSW. From the extensive literature survey, it has been observed that tool rotation speed, welding speed, tool profile and tool offset are the parameters which affect weld produced. Some work has been done to predict effect of parameters on weld but the effects of interaction need more attention. In present work, four parameters have been studied together and their interaction up to second order has been analyzed. Prior experiments were conducted to find the range of each parameter for which sound welds can be produced[36]. Each parameter has been examined at three levels for conveniently setting the parametric level on the machine. Face-centered central composite design (FCCCD) of response surface methodology (RSM) has been used to reduce the number of experiments. Destructive and non-destructive tests were carried out on the weld samples to get the insight of the weld. Tensile test and flexural test were conducted on the samples to get knowledge about the strength of the weld. Scanning electron microscope (SEM) image of the fracture surface has been studied to predict the type of fracture taken place during the tensile test of weld. Radiography test has been applied to detect any defects present in the weldment and also study material distribution in work piece after FSW. Vickers hardness of weld zone has been calculated to know the hardness of material in different regions.

2 Materials and Methods

2.1 Material of work piece and the tool

In the present study, aluminium 1060 alloy six mm thick sheet has been used as work piece. Cold rolled sheets of 6 mm thickness were cut to dimension 100 mm × 90 mm × 6 mm. The work pieces were cut for welding in such a manner that welding direction was perpendicular to the rolling direction of the sheet. Hence, the welded samples used for tensile and flexural strength tests were having the grain orientation direction of base material along the axis of the samples. To minimize defects in weld, it is required that during FSW the work piece should be in contact without any root gap. The surfaces of work piece which are kept in contact during FSW have been cut using Wire electrical discharge machining

(WEDM) to get a flat and smooth surface with no root gap. After this, the surface was rubbed with sandpaper followed by cleaning with acetone to remove oxides and impurities present on the surface.

Scanning electron microscopy (SEM)-Energy Dispersive Spectroscopy (EDS) (model: JEOL JSM-6048LV) has been used to identify the constituents of the material of work piece. Figure 1 shows the elements present in the work piece and their percentage. It is observed that 99.45 percent of the element is aluminium. The alloying elements found in the work piece are titanium, vanadium, chromium, manganese, iron, and zinc. During the FSW process, high stress is induced in the tool. The tool has been prepared with H-13 tool steel to get high strength and tool rigidity during welding. After the manufacturing of the tool, it was oil quenched to increase the hardness of the tool. For present work, three types of tools have been used for experimentation: threaded pin tool, straight pin tool and taper pin tool (Figure 2). The shoulder of each of the tool is 16 mm in diameter. The pin length is kept 5.7 mm for all the tools. 0.3 mm clearance is given to avoid any interference with the backing plate during welding. The straight pin tool is having the pin of diameter 6 mm throughout the length. The taper tool is made with the head of the pin as 5 mm and bottom as 10 mm. The threaded pin tool is made having 6 mm nominal diameter. Pin of each tool is given a slot on two sides to enhance the movement of the work piece material around tool pin.

2.2 Experimental procedure

The experiments were conducted on a CNC vertical axis milling machine with the suitable fixture and clamping. The tool was attached with the spindle of the machine which provides the rotational motion and the downward motion (Z-axis motion). Work piece was attached to the machine table which provided the transverse motion (Y-axis motion). The tool was inserted 5.8 mm into the work piece. The interference of 0.1 mm was given between tool shoulder and work piece to get better friction of tool with work piece during welding. After insertion of the tool, the tool was kept rotating in contact with work piece for ten seconds to rise work piece temperature. By this process, the work piece becomes soft and its plasticity increases.

The parameters which are investigated in the current study are tool rotation speed, welding speed, tool pin profile and offset of the tool from weld line. All these parameters have been studied at three levels to study their effect on weld produced. The parametric levels at which experiments are conducted are shown in Table 1. The experiments have been designed with face-centered central composite design (FCCCD) of response surface methodology (RSM) to perform the analysis with a reasonable number of experiments. Table 2 shows the experimental layout and different parametric combination at which experiment has been conducted. Total thirty runs of the experiment have been done. It consists of sixteen factorial points, eight axial points and six centre points in the experimental layout. This is to be noted that the axial distance is unity in the present FCCCD.

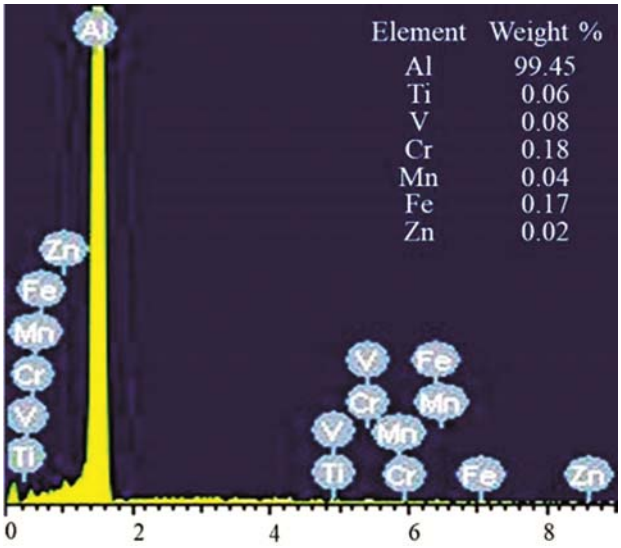

Fig. 1 — SEM-EDS detected element.

Fig. 2 — FSW tools used for the experiment.

Table 1— Properties of aluminium 1060 alloy.

Material properties	
Density	2.7 g/cc
Ultimate tensile strength (UTS)	120 MPa
Elastic modulus (Tensile)	68 GPa
Poisson‘s ratio	0.33
Thermal conductivity	230 W/m-K
Specific heat capacity	900 J/kg-K

Table 2 — Levels of parameters.

Coded value	Level 1-1	Level 20	Level 31
A-TRS (rpm)	700	1000	1300
B-WS (mm/s)	16	32	48
C-Tool pin profile	Threaded	Straight	Taper
D-Offset (mm)	-1	0	1

Threaded pin tool, straight pin tool, and taper pin tool are shown as -1, 0 and +1 respectively in the experimental layout. The insertion of the FSW tool centre away from weld line is represented as the offset of the tool. Depending on the tool rotation direction and welding direction there are two sides of work piece. They are known as advancing side and retreating side (Shown in figure 3). -1 indicates that the tool was inserted 1 mm towards advancing side, 0 shows that the tool was inserted at the weld line and +1 denotes that the tool was inserted 1 mm towards the retreating side. After completion of weld, visual inspection of weld samples has been done to identify any defect present on the surface. Surface roughness of the joint is measured. Radiography test has been performed on welds to study the material distribution and any defect present inside weld produced. Weld samples so obtained were cut perpendicular to the welding direction. From each weld specimen, three samples parts were cut for tensile test, flexural test and metallographic examination of weld. The tensile test and flexural test have been done according to ASTM E8M-04 standards and E290-14 standards respectively[37,38].

The tensile test and flexural test were performed with cross head movement speed of 0.5 mm/s. Design expert software has been used to analyze the significance of different parameters. After the completion of the tensile test, the surface morphology of fractured sample has been studied by SEM. The samples undergoing metallographic examination were polished as per standard metallurgical polishing process. Vickers hardness test has been conducted on weld areas of different weldment. Hardness has been calculated at 25 points on each sample. It has been done at difference of 1 mm including the weld center and 12 points on each side of weld center.

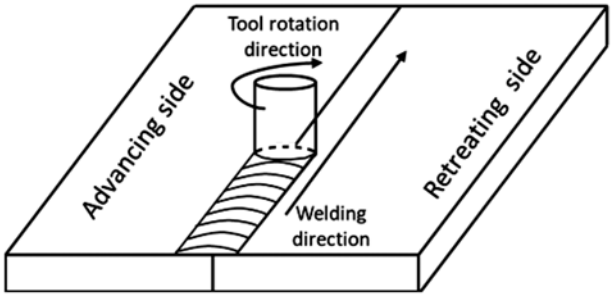

Fig. 3 — Schematic diagram of FSW process.

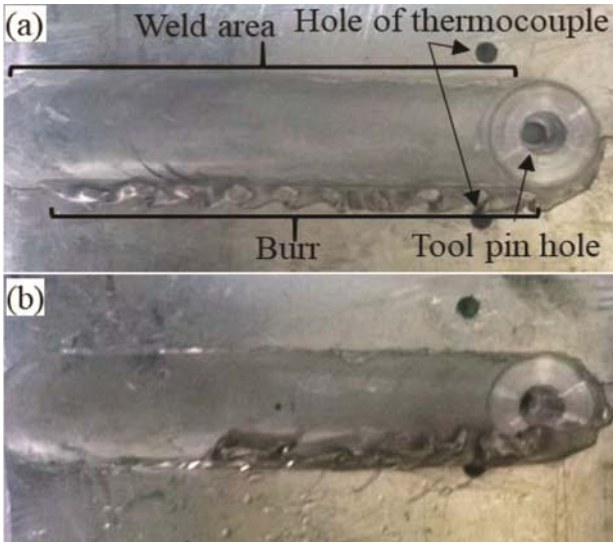

Fig. 4 — Weld surface of (a) weld 8 and (b) weld 16.

3 Results and Discussion

3.1 Visual inspection

Figure 4 (a and b) shows the surface of welds 8 and 16 respectively (Welding done with the parametric setting of experimental run N, as specified in Table 3, is represented as weld N). From the inspection, it was observed that the sheets have been successfully welded. No surface crack was found on any of the surface of the weld. Surface roughness of the weld area was found in range from 1.0 to 3.2 microns. Analysis of variance (ANOVA) indicates no significant dependence of the roughness with welding parameters. However, it was observed that roughness gradually increases from the start of weld towards the weld direction. All the blurs were formed on the retreating side of the weld whereas advancing side was blur free (Figure 4 (a and b)). The blur was mostly generated after a small travel of the tool. At

Table 3 — Experimental layout.

Exp. run	TRS (rpm)	WS (mm/s)	TPP	Off (mm)	UTS (MPa)	UFS (MPa)
1	-1	-1	-1	-1	73	219
2	+1	-1	-1	-1	85	208
3	-1	+1	-1	-1	83	236
4	+1	+1	-1	-1	96	202
5	-1	-1	+1	-1	78	216
6	+1	-1	+1	-1	76	188
7	-1	+1	+1	-1	68	217
8	+1	+1	+1	-1	86	178
9	-1	-1	-1	+1	91	200
10	+1	-1	-1	+1	99	226
11	-1	+1	-1	+1	82	205
12	+1	+1	-1	+1	96	202
13	-1	-1	+1	+1	84	200
14	+1	-1	+1	+1	83	210
15	-1	+1	+1	+1	69	199
16	+1	+1	+1	+1	80	204
17	-1	0	0	0	69	226
18	+1	0	0	0	78	205
19	0	-1	0	0	70	201
20	0	+1	0	0	75	206
21	0	0	-1	0	80	201
22	0	0	+1	0	71	188
23	0	0	0	-1	71	163
24	0	0	0	+1	65	157
25	0	0	0	0	72	192
26	0	0	0	0	70	185
27	0	0	0	0	71	195
28	0	0	0	0	66	186
29	0	0	0	0	72	189
30	0	0	0	0	74	189

the end of weld-travel, a hole was left as observed in Fig. 4. This is the area from where pin was retreated out. It is observed that typical fusion welding defects like porosity and unfilled crater were absent.

3.2 Radiography inspection

Radiography inspection is a non-destructive test used to get insight into the welded joint without destroying the part. This is widely used to detect any internal cracks and study the distribution of the material in the object. In radiography test, the area which has dark shade is the area that has least material concentration. Figures 5 (a and b) show the radiography test of weld 8 and 16, respectively. The burrs were removed before radiography using grinding process. From the image, it is observed that the material concentration is least in the path in which the tool pin passes along the weld line (pin

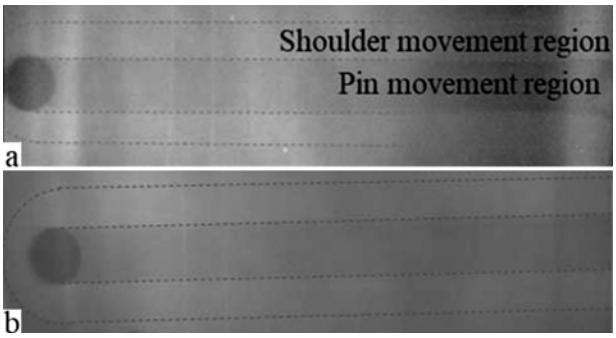

Fig. 5 — Radiography of (a) weld 8 and (b) weld 16.

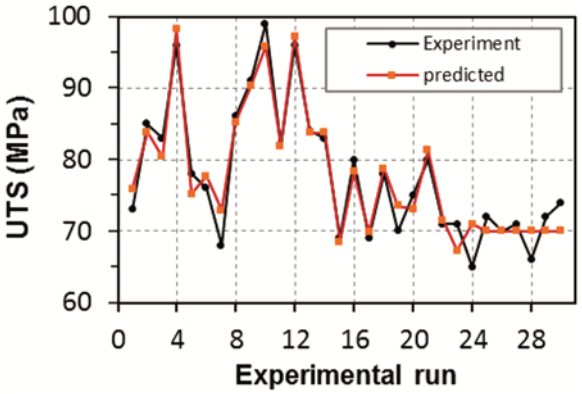

Fig. 6 — Variation of UTS with experimental run.

movement region (PMR)). This region is known as nugget region of the weldment. The area beside the dark area is shoulder movement region (SMR). This area is also specified as thermo-mechanically affected zone[6,14]. This area is the brightest of the other areas. This shows that it has more material concentration than other areas of the sheet. The material which has been pushed from PMR is accumulated in SMR. Hence, material concentration increases in SMR.

3.3 Tensile test

Table 3 shows the ultimate tensile strength (UTS) of the welds at different experimental runs. Highest UTS obtained is 99 MPa for the weld 10 with the strain percentage at peak was found to be 4.776. The lowest UTS is 65 MPa for the weld 24 with strain percentage at peak 0.8862. Figure 6 shows UTS of welds with respect to experimental run. A high variation in the UTS is observed from the graph. This indicates that the weld strength is dependent on the welding parameters. A further investigation of the effect of the parameters has been carried out through analysis of variance (ANOVA).

Table 4 shows the ANOVA table indicating the significance of different parameter on UTS.

Table 4 — ANOVA for UTS.

Source	Sum of Squares	df	Mean Square	F-Value	p-value Prob > F	
Model	2259.5	14.0	161.4	148.00	< 0.0001	significant
A- TRS	355.6	1.0	355.6	29.71	< 0.0001	significant
B- WS	0.8	1.0	0.8	0.07	0.7975	
C- TPP	429.9	1.0	429.9	35.91	< 0.0001	significant
D- Off	694.0	1.0	694.0	5.34	0.0355	significant
A×B- TRS × WS	96.6	1.0	96.6	8.07	0.0124	significant
A×C- TRS × TPP	30.0	1.0	30.0	2.50	0.1344	
A×D- TRS × Off	6.1	1.0	6.1	0.51	0.4868	
B×C- WS × TPP	47.0	1.0	47.0	92.00	0.0662	
B×D- WS × Off	166.9	1.0	166.9	195.00	0.0020	significant
C×D- TPP × Off	35.2	1.0	35.2	2.94	0.1070	
A2- TRS^2	46.9	1.0	46.9	92.00	0.0663	
B2- WS^2	28.0	1.0	28.0	2.34	0.1472	
C2- TPP^2	105.4	1.0	105.4	8.80	0.0096	
D2- Off^2	1.9	1.0	1.9	0.16	0.6946	
Residual	179.6	15.0	12.0			
Lack of Fit	144.4	10.0	14.4	2.05	0.2208	not significant
Pure Error	35.2	5.0	7.0		< 0.0001	
Cor Total	2439.0	29.0			< 0.0001	

During ANOVA analysis, the parameters which show lesser P value have higher significant effect on the UTS of weld. For the present study, 95 percent confidence level has been taken. It can be observed that different parameters have different level of significance on UTS. Tool rotation speed and tool pin profile are the most significant parameters followed by the offset of the tool from weld line. The interaction between the welding speed and offset of the tool from weld line is the most significant interaction. Second significant interaction is found between the tool rotation speed and welding speed. Hence, it can be concluded that welding speed itself is not a significant parameter but has an significant interaction with other parameters which can affect weld strength.

A regression model has been generated to predict the UTS of weld at different parametric setting. The regression equation with parametric value in coded form is given by Equation 1. The predicted value for the present experimental run is shown in figure 6. The relation between the experimental value and the predicted value is shown in Fig. 7. Correlation factor (R) and average relative percentage error (ARPE) for the analysis have been calculated using equation 2 and equation 3. It is found to be 0.962 and 2.63, respectively. Hence, it can be observed that the model can predict the value with accuracy.

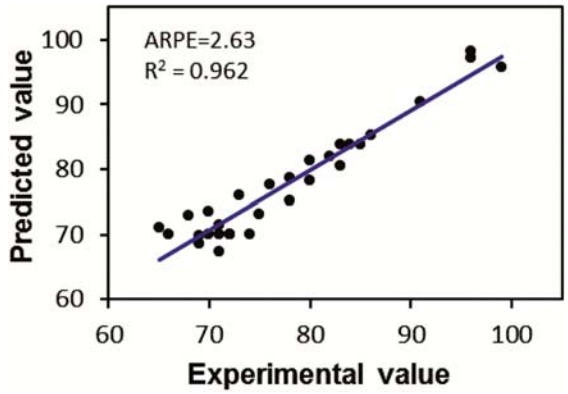

Fig. 7 — Relationship between the predicted value and the actual value of UTS.

$$UTS = 69.9919 + 4.4449\times A - 0.2129\times B - 4.89\times C + 1.8847\times D + 2.4573\times A\times B - 1.3687\times A\times C - 0.6166\times A\times D - 1.7135\times B\times C - 3.2302\times B\times D - 1.4833\times C\times D + 4.2564\times A^2 + 3.29\times B^2 + 6.38\times C^2 - 0.8603\times D^2 \quad \text{... (1)}$$

$$R = \frac{\sum_{i=1}^{N}\left(UTL_e^i - \overline{UTL_e}\right)\left(UTL_p^i - \overline{UTL_p}\right)}{\sqrt{\sum_{i=1}^{N}\left(UTL_e^i - \overline{UTL_e}\right)^2 \sum_{i=1}^{N}\left(UTL_p^i - \overline{UTL_p}\right)^2}} \quad \text{... (2)}$$

$$ARPE = \frac{1}{N}\sum_{i=1}^{N}\left|\frac{UTL_e^i - UTL_p^i}{UTL_e^i}\right| \times 100 \quad \text{... (3)}$$

Figure 8 shows a surface plot of the effects of tool rotation speed and welding speed on UTS of

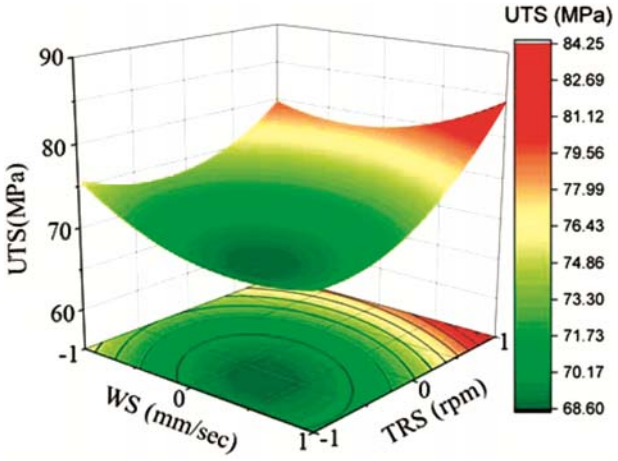

Fig. 8 — Surface plot for UTS with respect to tool rotation speed and welding speed.

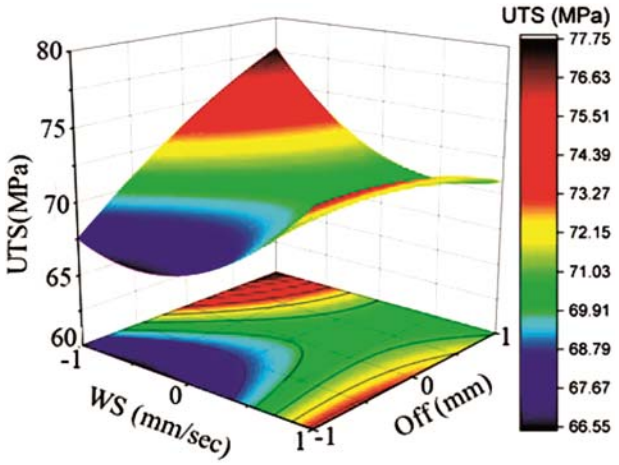

Fig. 9 — Surface plot for UTS with respect to welding speed and offset of the tool.

weldment. It is observed that UTS increases with increase in tool rotation speed, when other parameters are held constant. As the tool rotation speed increases, the increase in relative motion between the tool and work pieces enhances friction between the bodies and also increases the rate of breakage of bonds in work piece material. This increases the heat generation in the work piece[6]. Hence, the material of the work piece near the tool gets softens. This effect along with higher tool rotation speed leads to better mixing of work piece material. Mishra *et al.*[6] and Nandan *et al.*[14] have reviewed many research in the FSW field and have acknowledged that the softening and better mixing of material leads to higher strength of weld. The higher tool rotation speed also leads to grain refinement in the welding region[10]. All these effects lead to increase in weld strength. It is observed that increase of UTS with tool rotation speed is more pronounced at higher welding speed. At lower tool rotation speed, increase in welding speed leads to decrease in UTS but at higher tool rotation speed increase in welding speed leads to increase in welding strength. This is because at low tool rotation speed and high welding speed, the rise in temperature and mixing of material is less[6,19]. This leads to lower weld strength. However, at higher tool rotation speed, the mixing and temperature rise is obtained by high tool rotation speed. Therefore, mixing of the material and good welding strength can be achieved even if the welding speed is high. High tool rotation speed with high welding speed can lead to fine mixing of material. Hence, higher strength is observed.

Figure 9 shows the surface plot for the effect of welding speed and offset of the tool on UTS. At low

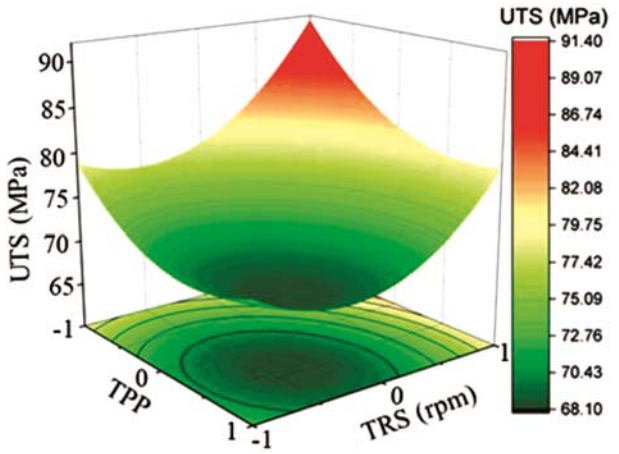

Fig. 10 — Surface plot of tool rotation speed and tool pin profile.

welding speed with offset towards retreating side, the UTS obtained is higher than the UTS obtained with offset towards the advancing side. However, at high welding speed UTS obtained is higher with offset towards advancing side, than UTS obtained with offset towards retreating side. Figure 10 shows surface plot for the effect of tool rotation speed and tool pin profile on UTS. The threaded pin tool (coded as -1) produces the weld with highest strength whereas straight pin tool (coded as 0) produces joint with lowest strength. Due to the thread on the surface of threaded pin tool, work piece material flow is better around the tool pin. This enhances the UTS of the weld produced by the threaded pin profile. The taper pin tool produces weld with moderate UTS. While conducting experiment, least vibration in the machine was experienced while welding with taper tool. The insertion of the tool in to work piece

and movement of the tool in work piece was smoother than with other pin tools. It is better to use taper pin tool for welding purpose if the machine's rigidity is low.

3.4 Surface morphology of fractured sample

The fractured surface of the welds 16 is shown in the Figure 11. The images show that three distinguished areas are formed on the fractured surface during the tensile test: Area 1, area 2 and area 3. Area 1 is the upper part of weld, area 2 is middle part and area 3 is the bottom part. During experimentation, it was observed that the crack was initially produced in the bottom part of the weldment and propagated towards the upper area resulting in fracture of the specimen.

Figure 12 shows the magnified image of area 1 in weld 16. It is observed that very fine dimple formations are present in this area. Fine dimple formation shows that this area is ductile in nature[6,14,24]. The shoulder of the tool comes in contact with top region of the work piece. Heat is generated in this area and conducts towards the downward side. Therefore, material gets the highest temperature and hence highest fluidity in this region. Higher fluidity with better mixing due to toll pin and shoulder leads to better mixing of material in this region. It has been reported the finest grain is observed in this region[24]. Due to the better mixing of the material and finer grains, high ductility is observed in this region.

Figure 13 shows magnified image of area 2 in weld 16. It is observed that dimples present in this region are bigger in size than the dimples in the area 1. The ductility of this area has been observed to be less as compared to upper area but more than the area 3.

High magnification image of area 3 is shown in Figure 14. A layer-by-layer surface is formed on fracture surface and no dimple formation was found in this area. A layer-by-layer formation shows that

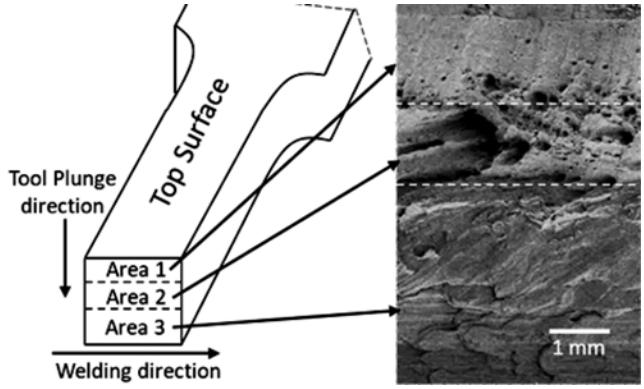

Fig. 11 — SEM image of fracture surface of weld 16.

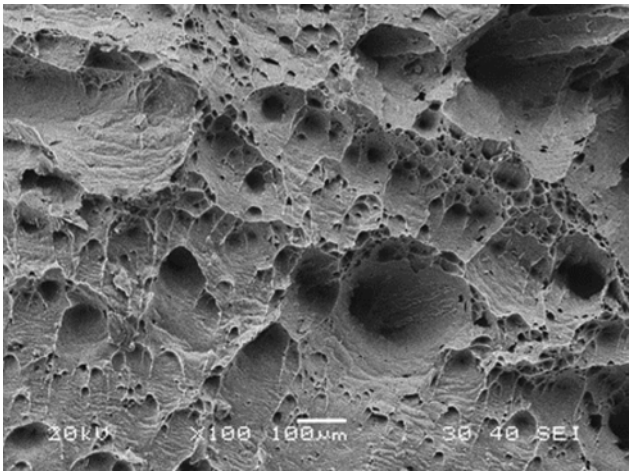

Fig. 13 — Magnified view of area 2 in weld 16.

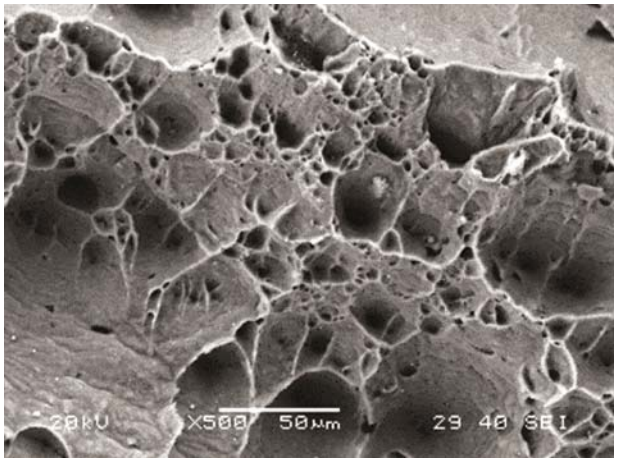

Fig. 12 — Magnified view of area 1 in weld 16.

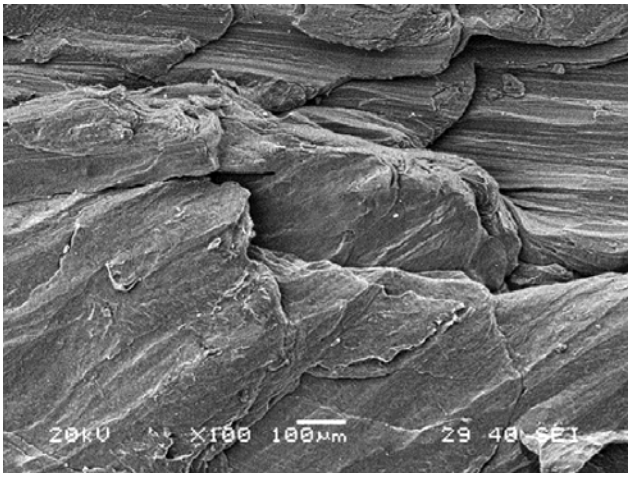

Fig. 14 — Magnified view of area 3 in weld 16.

this region is brittle in nature. In the lower area, the material is deposited when tool pin advances in the welding direction. So, in area 3, less mixing of material takes place in comparison to above area. Due to the less mixing of material, the ductility of the region is also low. Figure 15 shows the cross section view of weld 4 and weld 17. During the tensile test result analysis, it was observed that weld 4 has shown highest strength. On the other hand, weld 17 has shown one of the lowest strength. From the cross section fracture morphology, it is observed that in weld 4 the major part is area 1 and area 2. These regions are high strength ductile and semi ductile region respectively. This lead to high strength of weld 4. However, the proportion of area 1 & 2 in weld 17 is comparatively lower. The major portion being brittle region, this weldment shows lower strength and strain. Hence it can be observed that the UTS of the weldment is dependent on the presence of these regions. The weld having proportionally higher region of area 1 and area 2 shows higher strength. This weld also shows higher elongation during tensile test.

3.5 Flexural test

The flexural test has been conducted on all weld samples. Figures 16 (a) and 17(a) show the surface of the welds 8 and 28 respectively after the flexural test. It is observed that no crack is absent on the surface. Figures 16 (b) and Figure 17(b) show the side view of welds 8 and 28 respectively. From this, we can also observe that no cracks were formed after flexural test. From Figure 16 (b), it is observed that a tunnel defect is present in the weld. Such type of defect is common in FSW process[39]. The ultimate flexural strength achieved for welds obtained with different experimental runs are shown in Table 3.

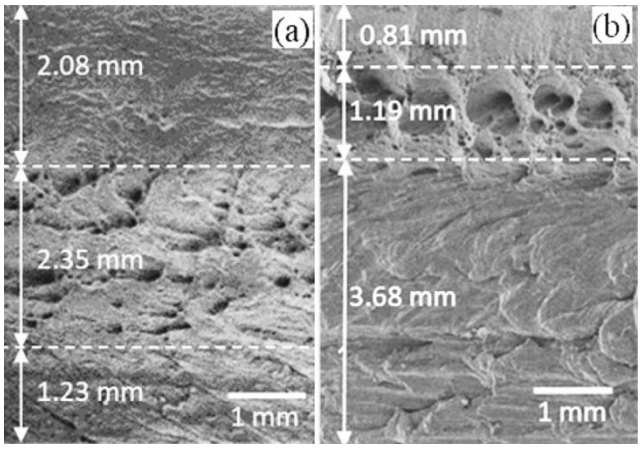

Fig. 15 — Fracture cross-section of (a) weld 4 and (b) weld 17.

Figure 18 shows the ultimate flexural strength (UFS) of different welds with different experimental run. The minimum UFS obtained is 158 MPa for weld 24 and maximum 236 MPa for weld 3. This shows that there is variation in UFS with a change in parameters. Further investigation on the effect of the parameters has been done with ANOVA analysis. Table 5 shows the ANOVA analysis for UFS. It can be concluded that tool rotation speed and tool pin profile are the significant parameters. The interaction between the tool rotation speed and offset of the tool is found to be the most significant interaction. Interactions of tool rotation speed and welding speed and tool pin profile and offset of the tool are also found to be significant interactions.

A regression model has been generated to predict the UFS of weld at different parametric setting. The regression equation with parametric value in coded form is given by Eq. 4. The relation between the

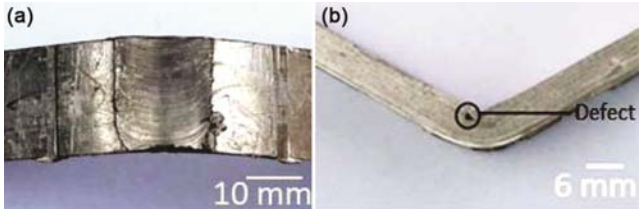

Fig. 16 — Views of weld 8 after flexural test (a) surface and (b) side.

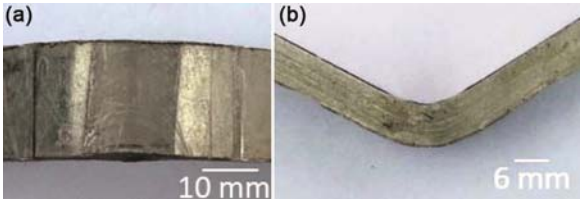

Fig. 17 — Views of weld 28 after flexural test (a) surface and (b) side.

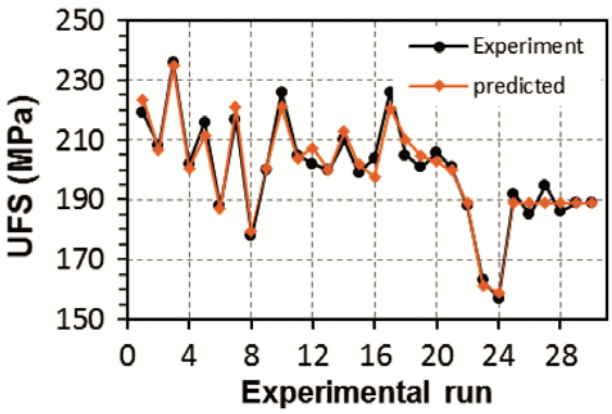

Fig. 18 — Variation in UFS with experimental run.

Table 5 — ANOVA for UFS.

Source	Sum of Squares	df	Mean Square	F Value	p-value Prob > F	
Model	8258.9	14	589.9	26.80	< 0.0001	significant
A- TRS	501.1	1	501.1	22.77	0.0002	significant
B- WS	17.5	1	17.5	0.79	0.3871	
C- TPP	535.0	1	535.0	24.31	0.0002	significant
D- Off	26.4	1	26.4	1.20	0.2907	
A×B- TRS × WS	292.2	1	292.2	127.00	0.0024	significant
A×C- TRS × TPP	56.1	1	56.1	2.55	0.1311	
A×D- TRS × Off	1415.1	1	1415.1	64.29	< 0.0001	significant
B×C- WS × TPP	2.4	1	2.4	0.11	0.7445	
B×D- WS × Off	55.8	1	55.5	2.53	0.1323	
C×D- TPP × Off	137.6	1	137.6	6.25	0.0245	significant
A^2- TRS^2	1827.2	1	1827.2	802.00	< 0.0001	
B^2- WS^2	560.3	1	560.3	25.46	0.0001	
C^2- TPP^2	75.7	1	75.7	44.00	0.0834	
D^2- Off^2	2150.4	1	2150.4	97.7	< 0.0001	
Residual	330.1	15	22.0			
Lack of Fit	261.7	10	26.2	1.91	0.2456	not significant
Pure Error	68.4	5	168			
Cor Total	8589.1	29				

experimental value and the predicted value is shown in figure 19. Correlation factor (R) and average relative percentage error (ARPE) have been calculated using equation 2 and equation 3. The values for the analysis is found to be 0.98 and 1.36 respectively. Hence, it can be observed that the model can predict the UFS with accuracy.

$$UFS = 189.00 - 5.28 \times A - 0.99 \times B - 5.45 \times C - 1.21 \times D - 4.27 \times A \times B - 1.87 \times A \times C + 9.40 \times A \times D - 0.39 \times B \times C - 1.87 \times B \times D + 2.937 \times C \times D + 26.56 \times A^2 + 14.71 \times B^2 + 5.41 \times C^2 - 28.81 \times D^2 \quad \ldots (4)$$

From the analysis, it can be observed that maximum flexural strength of 240 MPa can be obtained with parametric setting of 700 RPM tool rotation speed, 47 mm/s welding speed, threaded pin tool and 0.24 mm offset towards the retreating side. Figure 20 shows the surface plot for effect of tool rotation speed and welding speed on UFS. With increase of tool rotation speed, initially UFS decreases and then increases. Increase in the tool rotation speed causes finer deposition of material[6,14]. This is due to increase in turbulence of the material flow. Due to turbulence, there is irregular deposition of the material in the weld zone. This irregular deposition leads to decrease in UFS of the weld. Hence, UFS decreases with increase in tool rotation speed. However, with further increase in the tool rotation speed, lattice distortion and intra granular dislocation density also increases[40]. So, more number

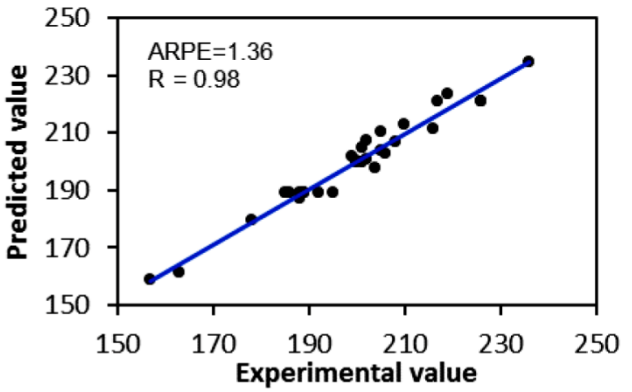

Fig. 19 — Relation between the predicted value and the actual value of UFS.

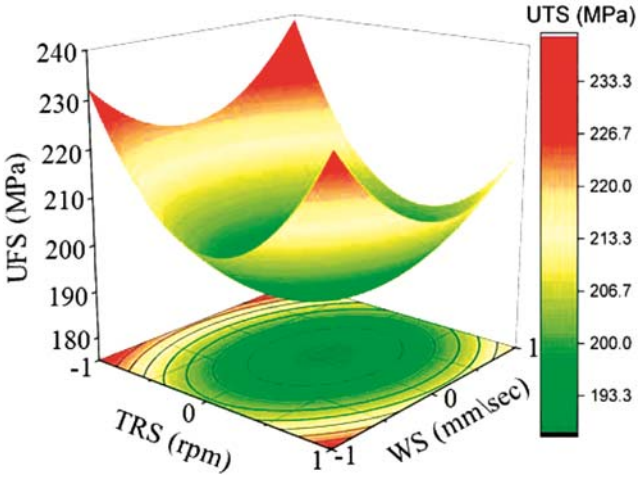

Fig. 20 — Surface plot for UFS with respect to tool rotation speed and welding speed.

of nucleation is produced during recrystallization that leads to large number of small grains. Finer grains formation and better mixing of material increases UFS of weld[6]. After a critical speed, this phenomenon gives more strength than the strength reduced due improper deposition by turbulence. Therefore, UFS increases with increase in tool rotation speed after a critical tool rotation speed.

Figure 21 shows the surface plot for effect of tool rotation speed and offset of the tool from weld line on UFS of the joint. Zero offset of the tool gives highest strength which means that the joint produced with tool inserting at the weld line produces highest strength joints. When tool is inserted at the centre, equal deposition takes place both in advancing and retreating side. Due to this, the flexural strength is more as no weak area is available for the bend to take place with less stress. The effect of offset of the tool is more pronounced at higher tool rotation speed than at lower tool rotation speed. Figure 22 shows surface plot for effect of tool pin profile and offset of the tool from weld line on UFS of joint. Threaded pin tool produces weld with highest UFS. Threaded pin profile mixes the material better due to the threads present on the pin. The threaded pin provides more surface area and path for the flow of material. Due to this, the weld produced is having finer mixing in comparison to weld produced with other pin type tools. In straight pin tool, flow of material is mainly due to the material pushed during the motion of the tool. So the mixing of the material of different sheets is not as good as in the case of threaded pin tool. Hence, the strength of the joint created with straight pin tool is less.

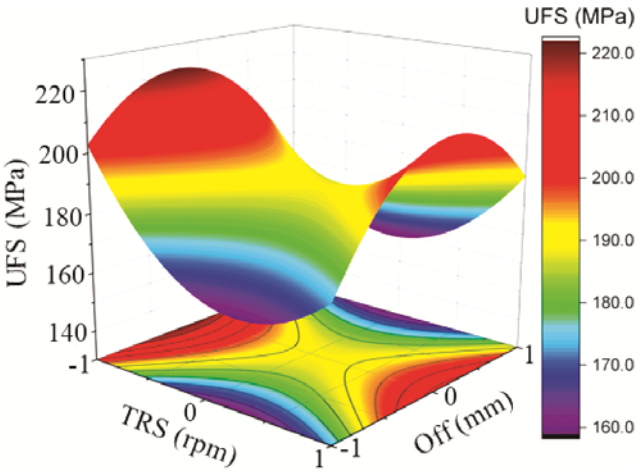

Fig. 21 — Surface plot for UFS with respect to tool rotation speed and offset of the tool.

3.6 Surface hardness

Vickers hardness has been measured at the cross section area of the weld (Fig. 23). Figure 23 shows the vickers hardness of welds 2, 5 and 21. Vickers hardness of the base sheet was calculated at six points and the mean was found to be 45.3 HV. It has been observed that vickers hardness of all the point in the weld is below the hardness of the base sheet. Zero in X-axis shows the centre of the weld. The negative value in X-axis shows the distance of the point in mm on the advancing side and positive value shows the distance towards the retreating side. It is observed that in the weld zone the centre part (nugget zone) has the lowest micro hardness. As material is pushed from the nugget zone towards the thermo-mechanically affected zone during the tool travel the material

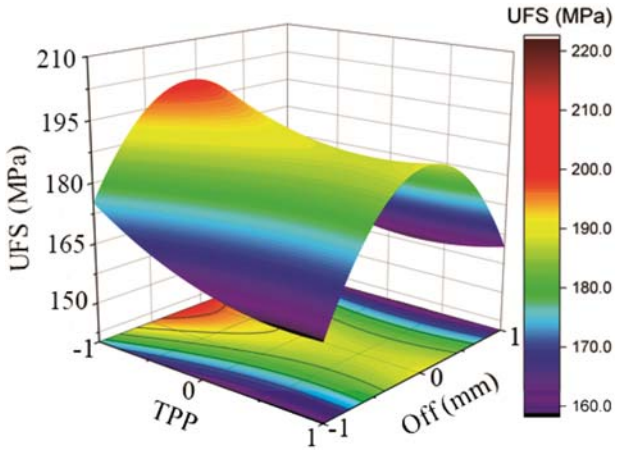

Fig. 22 — Surface plot of tool pin profile and offset of the tool.

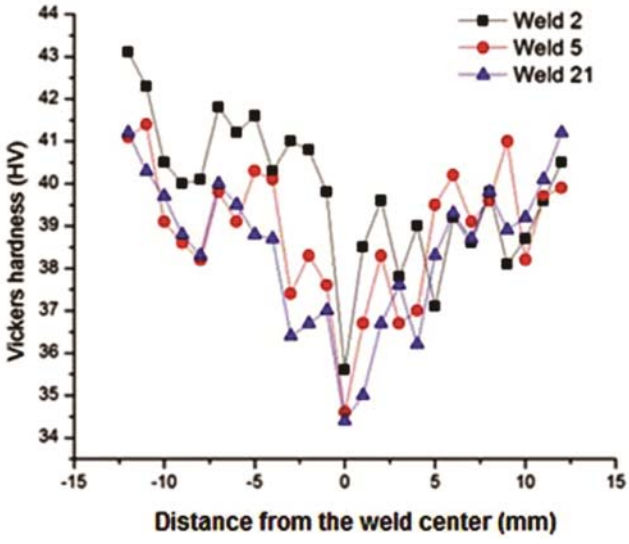

Fig. 23 — Surface hardness of weld 2, weld 5 and weld 21.

concentration is reduced in this area (discussed in section 3.2). Due to this phenomenon, the micro hardness is less.

After nugget zone there is rise in hardness. This region is the thermo-mechanically affected zone. It is observed that that the residual stress in thermo-mechanically affected zone is higher in comparison to nugget zone and heat affected zone[6,14,18]. Due to more material concentration and higher residual stress, higher micro hardness is observed in this region. After this region there is reduction in micro hardness as we move away from centre. Mishra *et al.*[6] and Singh *et al.*[41] have shown that in cross-section thermo-mechanically affected zone is followed by heat affected zone. Due to the thermal cycle during the FSW process softening takes place in this region. Hence, the micro hardness decreases in this region[14]. During the welding, the thermocouple was used to measure the temperature. It was observed that the temperature was reaching up to 480 °C. Due to heating, softening takes place in material. Hence, the material in this region becomes soft and shows less micro hardness.

4 Conclusions

Aluminium alloy 1060 six mm sheets have been successfully welded using FSW. The main conclusions drawn from the present study is summarized as follows:

(i) Tool rotation speed is the most significant parameter which affects the weld. The tensile strength increases with the increase in tool rotation speed. Higher heat generation and better mixing of the material enhances the tensile strength of the material.

(ii) Threaded pin tool is observed to produce weld having higher UTS and UFS than weld produced with straight pin tool and taper pin tool.

(iii) From the radiography test, it has been observed that least material concentration is observed in the nugget zone after the welding process. The area adjacent to nugget zone (thermo-mechanically affected zone) is found to have highest concentration of material.

(iv) From surface morphology of fractured surface, it can be concluded that the ductility of the weld is highest at the upper surface of the weld and decreases towards the bottom of the weld.

(v) The weldment having greater portion of ductile and semi ductile region shows more tensile strength and ductility.

(vi) The vickers hardness test shows that the welding zone has less hardness in comparison to the base material. The weld centre has the least hardness followed by heat affected zone. The hardness was found more towards the advancing side than in the retreating side.

References

1 Mathers G, *The Welding of Aluminium and its Alloys*, Woodhead Publishing, (2002) ISBN: 1 85573 567 9.

2 Heinz A, Haszler A, Keidel C, Moldenhauer S, Benedictus R & Miller W S, *Mater Sci Eng A*, 280 (2000)102.

3 Thomas W M & Nicholas E D, *Mater Des*, 18 (1997) 269.

4 Thomas W M, Nicholas E D, Needham J C, Murch M G, Templesmith P, & Dawes C J, GB Patent application no. 9125978.8. International patent No. PCT/GB92/02203 (1991).

5 Zhi- hong F U, Di-qiu H & Hong W, *J Wuhan University Technol –Mater Sci Edition*, 19 (2004) 61.

6 Mishra R S & Ma Z Y, *Mater Sci Eng: Reports*, 50 (2005)1.

7 Shrivastava A, Krones M & Pfefferkorn F E, *J Manuf Sci Technol*, 9 (2015)159.

8 Ericsson M & Sandström R, *Int J Fatigue*, 25 (2003)1379.

9 Li X W, Zhang D T, Cheng Q I U & Zhang W, *Trans Nonferrous Met Soc China*, 22 (2012) 1298.

10 Carlone P & Palazzo G S, *J Mater Process Technol*, 215 (2015) 87.

11 Khodaverdizadeh H, Mahmoudi A, Heidarzadeh A & Nazari E, *Mater Des*, 35 (2012) 330.

12 Da Silva J, Costa J M, Loureiro A & Ferreira J M, *Mater Des*, 51 (2013) 315.

13 Chen B, Ke C, Wei H, Zhiyuan L, Junshan Y, Lanting Z, & Aidang S, *J Mater Process Technol*, 223 (2015) 48.

14 Nandan R, DebRoy T & Bhadeshia H K D H, *Mater Sci*, 53 (2008) 980.

15 Zhang Z-k, Wang X-j, Wang P-c & Gang Z H A O, *Trans Nonferrous Met Soc China*, 24 (2014) 1709.

16 Xue P, Ni D R, Wang D, Xiao B L & Ma Z Y, *Mater Sci Eng A*, 528 (2011) 4683.

17 Dwivedi S P, *J Mech Sci Technol*, 28 (2014) 285.

18 Peel M A, Steuwer M, Preuss & Withers P J, *Acta Materialia*, 51 (2003) 4791.

19 Sakthivel T, G S Sengar & Mukhopadhyay J, *Int J Adv Manuf Technol*, 43 (2009) 468.

20 Hattel J H, Nielsen K L & Tutum C C, *Eur J Mech-A/Solids*, 33 (2012) 67.

21 Beygi R, Kazeminezhad M & Kokabi A H, *Trans Nonferrous Met Soc China*, 22 (2012) 2925.

22 Tan C W, Jiang Z G, Li L Q, Chen Y B & Chen X Y, *Mater Des*, 51 (2013) 466.

23 Donatus U G E T, Thompson G E, Zhou X, Wang J & Beamish K, *Mater Des*, 83 (2015) 203.

24 Xu W, Jinhe L, Hongqiang Z & Li F, *Mater Des*, 47 (2013) 599.

25 Li Z, Yumei Y, Shude J, Chai P & Ling W, *Mater Des*, 94 (2016) 368.

26 Su J-Q, Nelson T W, Mishra R & Mahoney M, *Acta Materialia*, 51 (2003) 713.

27 De Jesus J S, Loureiro A, Costa J M & Ferreira J M, *J Mater Process Technol*, 214 (2014) 2450.

28 Trueba J L, Georgina H, Daniel R & Lucie B J, *J Mater Proces Technol*, 219 (2015) 271.
29 Nandan R G G R, Roy G G, Lienert T J & Debroy T, *Acta Materialia*, 55 (2007) 883.
30 Seidel T U & Anthony P Reynolds, *Sci Technol Weld Joi*, 8 (2003) 175.
31 Seidel T U & Anthony P R, *Metall Mater Trans A*, 32 (2001) 2879.
32 Zhao Y-H, Lin S-B, Qu F-X & Wu L, *Mater Sci Technol*, 22 (2006) 45.
33 Schmidt Henrik N B, Dickerson T L & Jesper H H, *Acta Materialia*, 54 (2006)1199.
34 Guerra M, Schmidt C, McClure J C, Murr L E & Nunes A C, *Mater Charact*, 49 (2002) 95.
35 Buffa G, Hua J, Shivpuri R & Fratini L, *Mater Sci Eng A*, 419 (2006) 381.
36 Pandey A K, *Studies on Parametric Appraisal of Friction Stir Welding*, M.Tech dissertation, National Institute of Technology-Rourkela, Rourkela, India (2016).
37 ASTM International, E8/E8M-13 *Standard Test Methods for Tension Testing of Metallic Materials*, West Conshohocken, PA, 2013.
38 ASTM International, E290-14 *Standard Test Methods for Bend Testing of Material for Ductility*, West Conshohocken, PA, 2014.
39 Khan N Z, Arshad N S, Khan A Z & Suha K S, *J Alloys Comp*, 648 (2015) 360.
40 Xu W, Jinhe L, Guohong L & Chunlin D, *Mater Des*, 30 (2009) 3460.
41 Singh G, Singh K & Singh J, *Transactions Indian Institute Metals*, 64 (2011) 325.